

**Part 2**

**FULLERENES AND  
NANOTUBES**

# 11 Exploring the Concave Nanospace of Fullerenic Material

H. Kuzmany<sup>1</sup>, R. Pfeiffer<sup>1</sup>, T. Pichler<sup>1,2</sup>, Ch. Kramberger<sup>1</sup>,  
M. Krause<sup>2</sup> and X. Liu<sup>2</sup>

<sup>1</sup>*Institut für Materialphysik der Universität Wien, Wien, A*

<sup>2</sup>*Institut für Festkörper- und Werkstofforschung, Dresden, D*

## 1 INTRODUCTION

Network materials from pure carbon such as fullerenes and carbon nanotubes are excellent examples to explore nano-science and nano-technology on a molecular or low-dimensional solid state level. A lot of research work has been reported and was summarized in several review articles. Compared to this large volume of work rather little is known about the interior of the carbon cages. The reason is the fact that so far all attempts failed to open the fullerene cages and to inspect the interior chemically by studying reactions in the concave environment of the carbon atoms. Experimentalists were left with the cumbersome purification procedure of material where atoms were incidentally encaged during the growth process. Considerable progress was made recently at this point by detecting a possibility to fill at least the nanotubes with other molecules (Smith et al. 1998, Kataura et al. 2001) or more generally, with matter (Meyer et al. 2000). Particular interest at this point was recently dedicated to filling single wall carbon nanotubes (SWCNT) with C<sub>60</sub> fullerenes to make so called “peapods”.

We report in this contribution spectroscopic analyses of fullerenic carbon cages where other molecules or other cages are enclosed. The behavior of the filled material is compared with the behavior of the empty cages which allows to draw information on the interior of the cages. Results for both, filled fullerenes and filled SWCNT will be reported but the main emphasis is on the SWCNT side. In the former case the family of Re<sub>2</sub>@C<sub>84</sub> was selected where Re is one of the rare earth atoms Y or Sc. For these compounds the empty cage and the filled cage have the

same symmetry and therefore allowed a particular easy analysis. For SWCNT we studied the concentration of the  $C_{60}$  peas in the tubes and their reaction as a consequence of a doping with potassium.

## 2 EXPERIMENTAL

Higher fullerenes and endohedral fullerenes were prepared by arc discharge and subsequently subjected to an extended separation process by HPLC with a bucky clutcher column as described previously (Shinohara 2000, Krause et al. 2000). In the special case to be reported here as an example the isomer with  $D_{2d}$  symmetry was selected for the empty as well as for the filled cage. For the filling the set of diatomic rare earth metals  $Y_2$  and  $Sc_2$  as well as the four-atomic molecule  $Sc_2C_2$  (Wang 2001) were selected. All these molecules do not exist outside the cage but can be well prepared inside.

The SWCNT were prepared by laser desorption and finally cast into bucky paper. For the filling of the tubes with  $C_{60}$  the tubes were chemically treated first with hydrogen peroxide and then with hydrochloric acid in order to get rid of carbon particles and to allow access of the  $C_{60}$  cages to the interior of the tubes. Details of the preparation process were described by Kataura et al. (2001). All samples were equilibrated at 750 K for 12 hours in high vacuum before analysis.

Raman spectra were recorded with a Dilor xy spectrometer using up to 30 different laser lines for excitation and for a temperature range between 20 K and 500 K. In the case of the higher fullerenes and endohedral fullerenes the spectra were recorded from a thin film which was drop coated from a THF solution on a gold covered Si wafer. In the case of SWCNT and peapods the bucky paper was glued on a copper cold finger using silver paste.

Electron energy loss spectra (EELS) were recorded in a purpose built EELS spectrometer operated at 170 keV with an energy and momentum resolution of 160 meV,  $0.1 \text{ \AA}^{-1}$  respectively (Fink 1989). The high energy was appropriate to investigate the energy loss of the electrons when penetrating through a thin freestanding bucky paper film with 100 nm effective thickness.

## 3 ENDOHEDRAL FULLERENES

Figure 1 depicts the all over Raman response for the empty cage of  $D_{2d} C_{84}$  together with the low frequency part of the spectrum for two different dimetallo fullerenes. The very large number of lines in the former is a consequence of the large number of atoms in the cage and of the reduced symmetry. 155 Raman active fundamental cage modes can be expected which makes the detailed analysis of the spectrum cumbersome. The spectral range below  $200 \text{ cm}^{-1}$  is on the other hand free from lines.

Since we are interested in the dynamics of the encaged molecules it is this particular spectral range which is expected to be important. Part b of the figure displays the low frequency Raman response for two different dimetallo fullerenes together with the corresponding response from the empty  $D_{2d} C_{84}$  cage and the spectrum from  $C_{60}$ . As expected the latter two spectra exhibit a straight line without any signal. In contrast, the spectra for the dimetallo fullerenes exhibit an unexpected large number of lines. For  $Y_2C_{84}$  these lines are clearly grouped into quadruples. For  $Sc_2C_{84}$

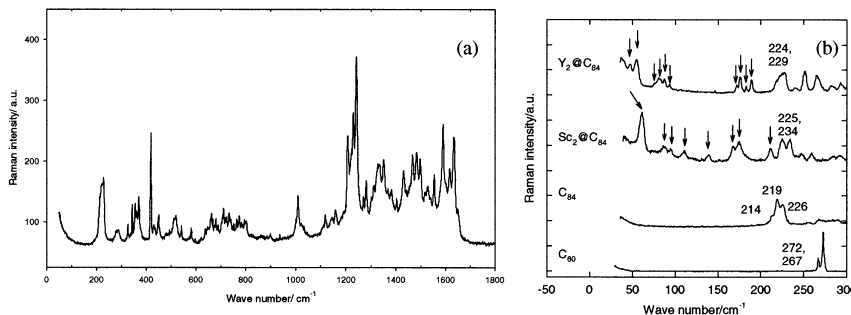


Fig. 1 Overall Raman spectrum of  $D_{2d} C_{84}$  (a), and low frequency part of the spectrum for two different dimetallo fullerenes; 90 K, 514.5 nm, 2 mW.

the number of extra lines is the same but the grouping is released. The total number of observed extra lines is 12 as compared to 4 ( $A_1$ ,  $B_2$ , and  $2E$ ) expected from a simple group-theoretical analysis.

The enhanced number of lines can be considered as a consequence of two effects. From a previous reported x-ray analysis the two rare earth atoms are expected to adopt symmetric positions on the  $S_4$  axis of the cage. As a consequence of the crystal field the site symmetry at this position is only  $C_1$  which means the degenerated E modes will split into two components with symmetry A and B. In addition the unit cell obviously consists of two dimetallo fullerene molecules. In this case Davydov splitting will result in a doubling of the lines if sufficient interaction between the molecules is provided. Since the cages and the enclosed metals are charged such interaction can indeed be expected to be strong. In the particular case of the diatomic ions in the  $D_{2d} C_{84}$  cage the symmetry does not allow dipole-dipole interaction. The quadrupole moment of the distributed charges is on the other hand reasonable and can account for the observed splitting of the lines. A detailed theoretical analysis of this interaction was worked out recently (Popov et al. 2001) and fully confirmed the above explanation.

## 4 C<sub>60</sub> PEAPODS

Peapods are a most interesting example of filling the interior of SWCNT with matter. Since carbon nanotubes as well as C<sub>60</sub> are very sensitive to Raman scattering the latter is a particularly useful technique to study these all carbon curved structures. Two questions appear to be of particular importance: What is the concentration of the fullerenes in the tubes and to what extent can the fullerene cages be doped inside the SWCNT cages.

### 4.1 Raman Response of SWCNT and C<sub>60</sub> Peapods

The Raman response of SWCNT has been extensively investigated in the recent past. There are several good reasons for this. The scattering cross section for selected lasers is unusually large. Resonance scattering from individual tubes or at least from bundles of tubes have been reported (Duesberg et al. 1999, Jorio et al. 2001). The radial breathing mode (RBM) around 180 cm<sup>-1</sup> exhibits a complicated line pattern as a consequence of a photoselective resonance scattering (Rao et al. 1997, Milner et al. 2000). The line position scales roughly as 1/d where d is the diameter of the nanotube. In detail the mean line positions (first spectral moments) as well as the widths of the lines (second spectral moment) exhibit an oscillatory behavior for excitation with different lasers. These oscillations originate from the macroscopic quantization of the transversal electronic states (Hulman et al. 2001). The so called D-line (defect induced line) around 1350 cm<sup>-1</sup> shifts with the energy of the exciting laser by 52 cm<sup>-1</sup>/eV, similar to the behavior of this line in graphite. In contrast to the latter material it exhibits also a superimposed oscillation like the RBM. The shift and the oscillation is a consequence of a double resonance scattering from phonons at the K-point of the Brillouin zone (Kürti et al. 2002). Finally also the so called G-line around 1590 cm<sup>-1</sup> provides insight into the electronic and lattice structure of the tubes. This line is related to the E<sub>2g</sub> line in graphite. Due to the more complex structure of the SWCNT the line consists of 6 components in the tubes. One of them couples strongly to the electrons in the metallic tubes and gives rise to a Fano-Breit-Wigner line shape for excitation which matches the first allowed transition in the metallic tubes.

Raman spectroscopy was expected to identify the C<sub>60</sub> molecules in the tubes. This is indeed the case as demonstrated in Fig. 2 where the spectra from a C<sub>60</sub> single crystal is compared with the response from the peapod system. The latter is blown up as to make the contribution from the peas observable. The almost full coincidence between the lines from C<sub>60</sub> in the single crystal and from the C<sub>60</sub> in the pods indicates that there is only weak interaction between the two systems. Even though, there is obviously enough driving force to suck the peas into the pods.

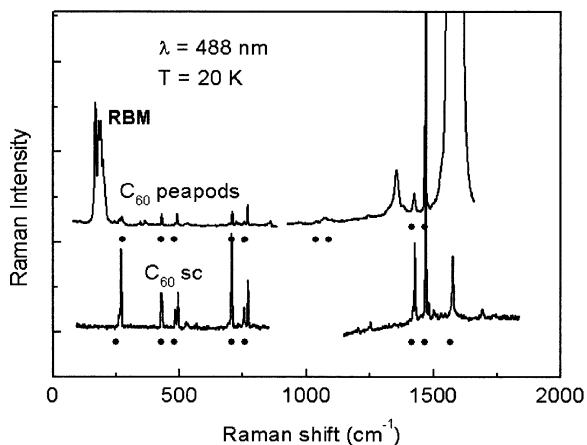


Fig. 2 Comparison of the Raman response from a peapod sample with the spectrum of single crystalline  $C_{60}$ . The intrinsically Raman allowed lines are marked. 20 K, 488 nm, 1 mW.

#### 4.2 The Concentration of Peas in the Tubes

A very often discussed question in the field is concerned with the degree of filling. Transmission electron microscopy (TEM) was most often used to demonstrate the filling of the tubes and to estimate the latter quantitatively. Whereas TEM is indeed an excellent method to demonstrate the filling it is not appropriate for a quantitative analysis. This results simply from the fact that it always evaluates selected areas. Raman spectroscopy would certainly be a more general method but unfortunately it does not allow to determine absolute values of concentrations. In addition the strong resonances for  $C_{60}$  and for the tubes require great care even for an evaluation of relative intensities.

Another promising bulk sensitive tool for the evaluation of the concentration is EELS. This technique was already demonstrated to provide a possibility for a quantitative analysis of the concentration for the peas in the pods (Liu et al. 2002). An example is given in Fig. 3. The recorded spectra for the transitions from the  $C1s$  level to the empty  $\pi^*$  or  $\sigma^*$  band of the peapods (spectrum pp) contain contributions from the carbons in the  $C_{60}$  molecule as well as from those in the tubes. Subtracting the corresponding spectrum of the pristine tubes (spectrum nt) allows to determine the concentration of carbons in the molecule as compared to the carbons in the tubes. This is possible provided that an appropriate scaling factor was used before subtraction. The scaling factor must be chosen in a way as to provide an optimum match between the difference spectrum and the EELS response from a  $C_{60}$  molecule in the range above the  $\sigma^*$  edge at 292 eV. In this energy range the  $C_{60}$

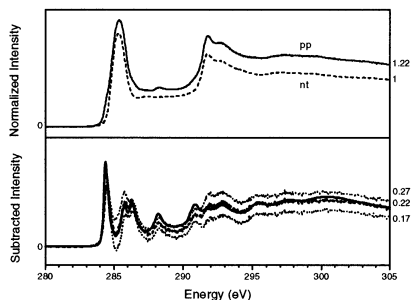


Fig. 3 EELS C1s spectra for pristine SWCNT (nt), peapods (pp), and difference between (pp) and (nt) generated with different scaling factors. The thick solid line in the lower panel is the C<sub>60</sub> reference.

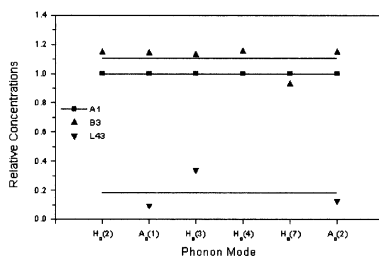


Fig. 4 Relative concentration of C<sub>60</sub> in SWCNT for three different samples as evaluated from 6 relevant C<sub>60</sub> Raman lines.

signal is hardly altered by the chemical environment. In the case of Fig. 3 this was achieved with a scaling factor of 1.22. For a completely filled system with an observed C<sub>60</sub>-C<sub>60</sub> distance of 0.97 nm and a tube diameter of 1.36 nm the ratio between carbons in C<sub>60</sub> and carbons in the tubes is 0.37. Thus the observed scaling factor is consistent with a filling of 60%. As C<sub>60</sub> can only enter tubes with a minimum diameter of estimated 1.3 nm (molecule diameter plus 2 times van der Waals distance in graphite) the percentage of filling for tubes with a large enough diameter is even higher.

To determine the concentration of the peas in the pods by Raman is straight forward. One has to consider the relative intensities between the response from the SWCNT and from the peas. This can be evaluated for various laser lines and for all significant Raman allowed modes of the peas. The technique has the advantage that the Raman analysis of the radial breathing mode yields simultaneously the mean tube diameter and the width of the diameter distribution. Of course the intensity ratios can only provide a relative concentration as the response for the different lasers and for the different Raman lines has to be calibrated. Figure 4 yields the result for three samples. Sample A1, for which the EELS analysis is presented in Fig. 3, was used for calibration. The measured intensity ratios between RBM response and C<sub>60</sub> response was considered A1 for the 60% filled sample. The concentrations evaluated for the other two samples exhibit slightly higher concentration for the sample B3 and a much lower concentration for the sample L43. Even though the concentrations evaluated for the different Raman lines exhibit a considerable scattering the large number of probe lines yields finally a rather low mean error for the analysis. For the three samples evaluated the results obtained from the Raman analysis was 60% filling for A1 (as calibrated from EELS), 67% for B3 and 11% for L43. The corresponding values from EELS are 60% for A1, 67% for B3 and 20% for L43.

### 4.3 Doping the Peas Inside the Tubes

As  $C_{60}$  is known to provide interesting physical properties such as a metallic or polymeric state or even superconductivity for certain doping concentrations, the doping process was a challenging object of research. Peapods were therefore exposed to an atmosphere of hot potassium vapor in a cryostat. The Raman response of the whole spectrum and the change of conductance were *in situ* recorded after different times of exposures. Characteristic changes in the frequency range of the tangential modes were recorded as depicted in Fig. 5a. Excitation was performed

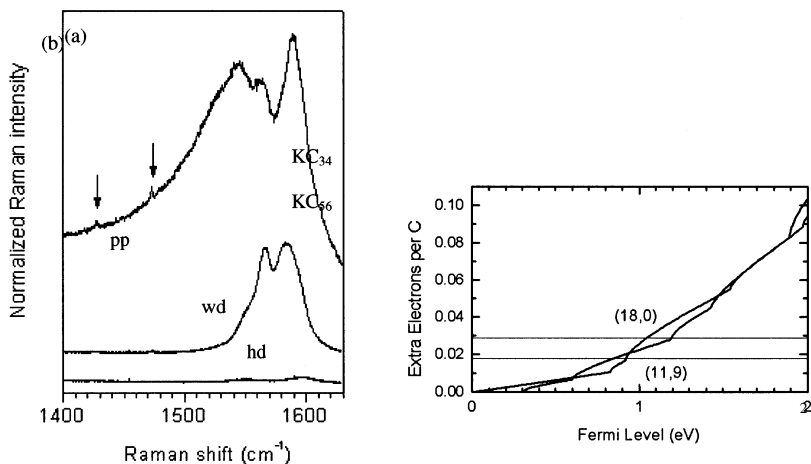


Fig. 5 Raman response of the tangential modes for pristine peapods and after various stages of the doping process (20 K, 640 nm, 2 mW) (a). (pp) holds for the pristine peapods, (wd) for the weakly doped system and (hd) for the heavily doped material. Part (b) exhibits the calculated shift of the Fermi level with increasing concentration of electrons per carbon.

with a red laser to stress the response from the metallic tubes. The broad Fano-Breit-Wiegner response is obvious for the undoped samples (spectrum pp). Weak doping leads already to a dramatic reduction of the response of the Fano line. This indicates that the resonance transition is lost due to filling up of the states in the first van Hove singularity of the metallic tubes. In order to estimate for which concentration this may occur we have plotted in Fig. 5b the relation between the shift of the Fermi level with the charge per carbon for two different tubes. One of them is metallic, the other one is semiconducting. For the evaluation a tight binding approximation was used. The lower dashed horizontal line marks the filling of the first van Hove singularity for the metallic tubes. The resonance is expected to be lost when the



states in the peak of the density of states are filled. The corresponding concentration of charge is  $C^{-0.018}$  or  $KC_{56}$ .

Continuing the exposure we eventually reach the heavily doped state where also the response from the graphitic lines of the tubes have disappeared. In other words, now also the corresponding van Hove singularities from the semiconducting tubes were filled up and resonance transitions are not any more possible. The intensity of the spectrum has decreased by almost a factor of 100. Considering again the filling of the states the upper dashed horizontal line in Fig. 5b indicates the concentration of extra electrons per carbon for which the third van Hove singularity in the semiconducting tubes which is responsible for the resonance becomes filled. The evaluated concentration is in this case  $C^{-0.03}$  or  $KC_{33}$ . This concentration is lower than a value determined from an EELS analysis from which  $KC_{10}$  was derived. Similarly, for the fully doped state of graphite (stage 1) a concentration  $KC_8$  was reported. The discrepancies may either result from the shortcomings of the tight binding model in the case of high doping known as nonrigid band structure effects or from a noncomplete charge transfer for the heavily doped state. In fact a discrepancy between the structurally determined concentration of the dopant atoms and the filling of tight binding bands is also known for graphite.

Further information on the heavily doped state can be drawn from blowing up the response from the G-line (curve (hd) in Fig. 5a). The response from the pentagonal pinch mode of  $C_{60}$  remains observable but appears downshifted by  $40\text{ cm}^{-1}$ . This means the  $C_{60}$  molecules became charged by about 6 electrons and are thus formally in an ionic state of  $C_{60}^{-6}$ .

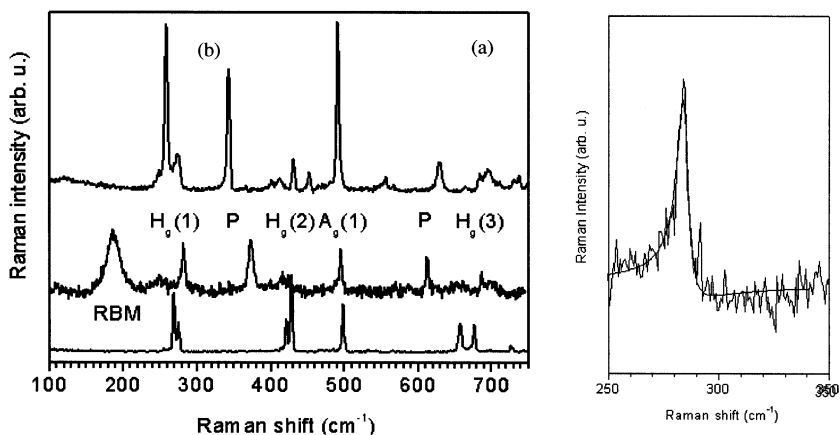


Fig. 6 Radial part of the Raman spectrum for heavily doped peapods ((a) center) as compared to the response from crystalline  $C_{60}^{-6}$  ((a) bottom) and for the doped polymer  $RbC_{60}$  ((a) top). Part b depicts the line shape analysis for the  $H_g(1)$  mode for the doped phase.

Finally, also the response from the radial modes yields information on the structure the peas adopted eventually. Figure 6 depicts spectra between 100 and 700  $\text{cm}^{-1}$  for the heavily doped peapod system in comparison to the spectrum for  $\text{C}_{60}^{-6}$  in the crystalline phase and a spectrum from a polymeric phase of doped  $\text{C}_{60}$ . It is obvious from the figure that the characteristic lines from crystalline  $\text{C}_{60}^{-6}$  are recovered in the heavily doped peapod system but in addition two strong lines at 370  $\text{cm}^{-1}$  and at 625  $\text{cm}^{-1}$  appear. From a comparison with the spectrum recorded for the polymeric phase  $\text{RbC}_{60}$  where the corresponding lines appear at 335 and 620  $\text{cm}^{-1}$ , respectively, the structure of the charged peas in the pods can be safely assigned to a linear polymeric phase. According to a calculation of Pekker et al. (1998) for a  $\text{C}_{60}$  cage with charge  $-6$  the single bonded polymer is expected to be much more stable as compared to the double bonded linear chain. Accordingly we conclude that the charged molecules in the tubes polymerize to a single bonded linear chain. This result is unique in a sense that such a polymer has not been observed so far outside the tubes.

There is some more information from Fig. 6a. The scattering intensity from the RBM has strongly decreased and is now approximately equal to the scattering intensity from the fullerene lines. Further on, when we excite the radial part of the spectrum from the doped peapods the oscillatory behavior is completely quenched and the width of the RBM response is in quantitative agreement with the width of the diameter distribution determined before from a Raman analysis. All this is consistent with the above mentioned loss of resonance transitions as a consequence of the filling the states up to the third van Hove singularities for the semiconducting tubes. Finally the line of the  $\text{H}_g(1)$  modes exhibits a clear Fano-Breit-Wiegner shape which is explicitly demonstrated in Fig. 6b, together with a fitted line pattern. Since this line originates from the molecules inside the tubes it is evident that the charged  $\text{C}_{60}$  molecules participate in the metallic state of the tubes. This result nicely confirms a recent calculation of Okada et al. (2001) in which the authors demonstrated that states from the  $\text{C}_{60}$  split off and merge with the conduction band of the tubes.

## 5 SUMMARY

Summarizing we have demonstrated that the interior of the new fullerene carbon cages provides an interesting nanoscale reactor for new materials and compounds which do not exist in the outside world. This is demonstrated explicitly from an analysis of dimetallo fullerenes where the Raman spectra give evidence for a strong bonding between the two rare earth ions inside the cage and the carbon atoms of the cage. The crystal field inside the cages reduces the local symmetry at the position of the rare earth atoms and a quadrupole interaction between the charged entities yields a doubling of the number of metal-cage modes.

In the case of  $C_{60}$  inside SWCNT the oscillatory behavior of the first and second moment of the response of the RBM is retained as long as the tubes are not charged. The concentration of the peas can be determined from the difference of EELS spectra recorded for peapod systems and for empty tubes of the same batch. Raman scattering allows to determine a relative concentration of  $C_{60}$  in the tubes from a comparison of intensities of Raman lines from the tubes and from the peas.

Doping the peapod system with electron acceptors quenches the resonance excitation from the tubes and the quantum oscillations for the RBM. Electrons are transferred to the cage of the tubes and to the cages of the  $C_{60}$  molecules inside the tubes. For the latter a charge state up to  $C_{60}^{-6}$  is reached. In this state the carbon cages establish single covalent bonds and form a linear polymeric chain with metallic character.

## ACKNOWLEDGEMENT

The authors acknowledge the supply of samples from H. Shinohara, University of Nagoya, H. Kataura from the Tokyo Metropolitan University and from L. Dunsch, Institut für Festkörperphysik und Werkstofforschung, Dresden. Financial support from the Fonds zur Förderung der Wissenschaftlichen Forschung in Österreich, projects P14386 and P14146 and from the European community, project FULPROP is appreciated.

## REFERENCES

- Duesberg, G. S., Blau, W. J., Byrne, H. J., Muster, J., Burghard, M. and Roth, S., 1999, Experimental observation of individual single-wall nanotube species by Raman microscopy. *Chemical Physics Letters*, **310**, pp. 8–14.
- Fink, J., 1989, Recent Advances in Electron Energy Loss Spectroscopy. *Advances in Electronic Electron Physics*, **75**, pp. 121–240.
- Hulman, M., Plank, W. and Kuzmany, H., 2001, Distribution of spectral moments for the radial breathing mode of single wall carbon nanotubes. *Physical Review B*, **63**, pp. 081406-1–081406-4.
- Jorio, A., Saito, R., Hafner, J. H., Lieber, C. M., Hunter, M., McClure, T., Dresselhaus, G. and Dresselhaus, M. S., 2001, Structural ( $n, m$ ) Determination of Isolated Single-Wall Carbon Nanotubes by Resonant Raman Scattering. *Physical Review Letters*, **86**, pp. 1118–1121.
- Kataura, H., Maniwa, Y., Kodama, T., Kikuchi, K., Hirahara, K., Suenaga, K., Iijima, S., Suzuki, S., Achiba, Y. and Krätschmer, W., 2001, High-yield fullerene encapsulation in single-wall carbon nanotubes. *Synthetic Metals*, **121**, pp. 1195–1196.

- Krause, M., Hulman, M., Kuzmany, H., Kuran, P., Dunsch, L., Dennis, T. J. S., Inakuma, M. and Shinohara, H., 2000, Low-energy vibrations in  $\text{Sc}_2\text{@C}_{84}$  and  $\text{Tm@C}_{82}$  metallofullerenes with different carbon cages. *Journal of Molecular Structure*, **521**, pp. 325–340.
- Kürti, J. et al., 2002, *Physical Review B (in press)*.
- Kuzmany, H., Plank, W., Hulman, M., Kramberger, Ch., Grüneis, A., Pichler, Th., Peterlik, H., Kataura, H. and Achiba, Y., 2001, Determination of SCWNT diameters from the Raman response of the radial breathing mode. *The European Physical Journal B*, **22**, pp. 307–320.
- Liu, X., Pichler, T., Knupfer, M., Golden, M. S., Fink, J., Kataura, H., Achiba, Y., Hirahara, K. and Iijima, S., 2002, Filling factors, structural, and electronic properties of  $\text{C}_{60}$  molecules in single-wall carbon nanotubes. *Physical Review B*, **65**, pp. 045419-1–045419-6.
- Meyer, R. R., Sloan, J., Dunin-Borkowski, R. E., Kirkland, A. I., Novotny, M. C., Bailey, S. R., Hutchison, J. L. and Green, M. L. H., 2000, Discrete Atom Imaging of One-Dimensional Crystals Formed Within Single-Walled Carbon Nanotubes. *Science*, **289**, pp. 1324–1326.
- Milnera, M., Kürti, J., Hulman, M. and Kuzmany, H., 2000, Periodic Resonance Excitation and Intertube Interaction from Quasicontinuous Distributed Helicities in Single-Wall Carbon Nanotubes. *Physical Review Letters*, **84**, pp. 1324–1327.
- Okada, S., Saito, S. and Oshiyama, A., 2001, Energetics and Electronic Structures of Encapsulated  $\text{C}_{60}$  in a Carbon Nanotube. *Physical Review Letters*, **86**, pp. 3835–3838.
- Pekker, S., Oszlányi, G. and Faigel, G., 1998, Structure and stability of covalently bonded polyfulleride ions in  $\text{A}_x\text{C}_{60}$  salts. *Chemical Physics Letters*, **282**, pp. 435–441.
- Popov, N. et al., 2001, unpublished.
- Rao, A. M., Eklund, P. C., Bandow, S., Thess, A. and Smalley, R. E., 1997, Evidence for charge transfer in doped carbon nanotube bundles from Raman scattering. *Nature*, **388**, pp. 257–259.
- Shinohara, H., 2000, Endohedral metallofullerenes. *Reports on Progress in Physics*, **63**, pp. 843–892.
- Smith, B. W., Monthieux, M. and Luzzi, D. E., 1998, Encapsulated  $\text{C}_{60}$  in carbon nanotubes. *Nature*, **396**, pp. 323–324.
- Wang, C.-R., Kai, T., Tomiyama, T., Yoshida, T., Kobayashi, Y., Nishibori, E., Takata, M., Sakata, M. and Shinohara, H., 2001, A Scandium Carbide Endohedral Metallofullerene:  $(\text{Sc}_2\text{C}_2)\text{@C}_{84}$ . *Angewandte Chemie*, **113**, pp. 411–413.